ELSEVIER

Journal of Molecular Catalysis A: Chemical 119 (1997) 393–403

JOURNAL OF MOLECULAR CATALYSIS A: CHEMICAL

Theoretical characterization of iron and manganese porphyrins for catalyzed saturated alkane hydroxylations

Francisco Torrens

Departament de Química Física, Facultat de Química, Universitat de València, Dr. Moliner 50, E-46100 Burjassot (València), Spain

Received 4 June 1996; accepted 10 July 1996

Abstract

The theoretical characterization of porphin (H_2Por), iron and manganese porphyrins M^{III}(Por) and their chlorine derivatives M^{III}(Por)Cl has been carried out. This work represents a first step for modelling catalyzed saturated alkane hydroxylations. The chlorine atom is responsible for the existence of a dipole moment of 1.2–2.0 D in the M^{III}(Por)Cl molecules and for a negative value of the mean quadrupole moment (-16–(-14)DÅ). The charge of the metal atom (1.8–2.2 *e*) is rather varied (to 2.1–2.6 *e*) and the effective polarizability (2.8–2.9 Å^3) is increased (to 3.5–3.6 Å^3) by the addition of the chlorine atom. Starting from the porphin molecule, the presence of the metal atom decreases the molecular volume, molecular surface area and solvent accessible surface area. The addition of the chlorine atom increases these geometrical descriptors. The fractal dimension for the metal atom solvent accessible surface takes a very high value of 6.1–6.2 when compared with the molecular value averaged for non-buried atoms ($D' = 1.44$). This means that the irregularity of the molecular surface is maximal at the metal atom solvent accessible surface. The *n*-octanol–water partition coefficient is minimal for the metal free porphin (log $P = 5.48$) and maximal for the non-charged chlorine porphyrin derivative (log $P = 6.19$).

Keywords: Porphyrin; Hydroxylation; Multipole moments; Net charges; Polarizability; Geometrical descriptors; Topological indices; Fractal dimension; Solubility; Partition coefficient

1. Introduction

Saturated alkane hydroxylations are catalyzed by cytochrome P-450 enzymes [1] and by iron and manganese tetraarylporphyrin complexes [2]. Both enzymatic and biomimetic hydroxylations involve the oxidative cleavage of a C–H bond by a high-valent metal-oxo species as the rate-determining step in alcohol formation [3]:

$$M^{III}(Por)X \rightarrow \left[(Por)M^{V}=O \leftrightarrow (Por^{\cdot+})M^{IV}=O\right]$$

where M = Fe, Mn and X = Cl.

In this paper we present the theoretical characterization of the H_2Por, M^{III}(Por) and M^{III}(Por)Cl molecules (see Fig. 1). This work represents a first step for modelling catalyzed saturated alkane hydroxylations.

2. Electrostatic properties

We have written a program called POLAR for the theoretical simulation of molecular electrostatic properties and polarizability. Atomic net charges and polarizabilities are calculated

PII S1381-1169(96)00503-1

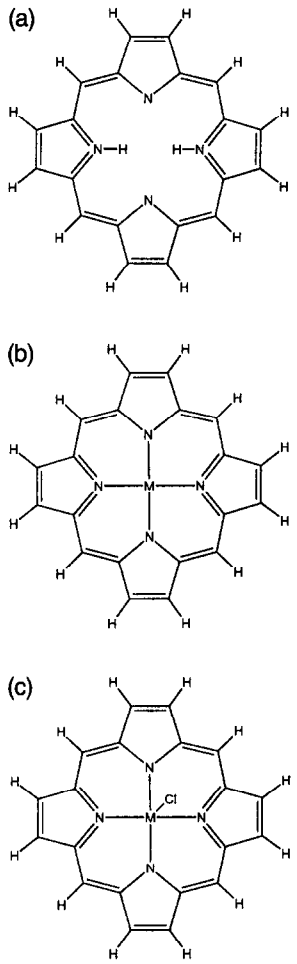

Fig. 1. Molecular structures of (a) porphin (H_2Por), (b) M^{III}(Por) and (c) M^{III}(Por)Cl molecules.

from their σ and π contributions [4,5]. σ net charges and polarizabilities are estimated by the principle of electronegativity equalization [6,7] but applied bond by bond in the molecule [4,5]. π net charges and polarizabilities are evaluated with the method of Hückel. Dipole, $\overline{\mu}$, and tensor quadrupole, $\overline{\overline{\Theta}}$, moments are calculated from the point (atomic) distribution of net charges. A right-handed inertial axis system is used to identify the tensor components. The inertial axes, in the order of increasing moments of inertia, are used for the Cartesian axes x, y, z.

In describing the partial charge method developed for the Mulliken scale [8], Huheey [9] has mentioned that most elements approximately double their (Mulliken) electronegativities as the partial charge approaches +1 whereas their electronegativities essentially disappear (approach zero) as the partial charge approaches −1. The Mulliken and Pauling scales are roughly proportional, so Huheey's observation may be expressed in Pauling units as [7]

$$X_{eq} = X_A + \Delta_A X_A$$

or

$$\Delta_A = \frac{X_{eq} - X_A}{X_A}$$

Here, X_{eq} is the electronegativity as equalized through Sanderson's principle. X_A is the initial, pre-bonded electronegativity of a particular atom A and Δ_A is the σ partial charge on A. Charge conservation leads to a general expression for X_{eq}:

$$X_{eq} = \frac{N + q}{\sum_{\text{atoms}} \nu_A / X_A}$$

where $N = \Sigma\nu$ equals the total number of atoms in the species formula and q is the σ molecular charge.The σ partial charge Δ_A on atom A can be generalized as

$$\Delta_A = \sum_{\text{bonds}} \frac{X_{eq,b} - X_A}{X_A}$$

and the electronegativity equalized for bonds is given as

$$X_{eq,b} = \frac{2 + q/m}{1/X_A + 1/X_B}$$

where m is the number of bonds in the molecule.

Sanderson's principle allows the calculation of the σ atomic polarizabilities (equalized bond by bond) as

$$\alpha_A = \frac{\partial \Delta_A}{\partial X_A} = \sum_{\text{bonds}} \times \frac{(1 + L_A - \Delta_A)(2 - q/m) X_B}{(2 + L_A + L_B - \Delta_A - \Delta_B)(X_A + X_B)^2}$$

where the coefficients $(1 - \Delta_A)$ and $(2 - \Delta_A - \Delta_B)$ have been corrected to take into account the number of lone pairs on atoms A and B, L_A and L_B, respectively. π atomic net charges and polarizabilities are calculated with the Hückel molecular orbital (HMO) theory and added to the σ parts: $\Delta = \Delta_\sigma + \Delta_\pi$ and $\alpha = \alpha_\sigma + \alpha_\pi$. The calculation of dipole and quadrupole moments from the point (atomic) distribution of net charges $(\sigma + \pi)$ has been reported elsewhere [4,5].

3. Interacting induced dipoles polarization model for molecular polarizabilities

The calculation of molecular polarizabilities has been carried out by the interacting induced dipoles polarization model [10–12] that calculates tensor effective anisotropic point polarizabilities by the method of Applequist [13,14].

One considers the molecule as being made up of N atoms (represented by i, j, k, ...), each of which acts as a point particle located at the nucleus and responds to an electric field only by the induction of a dipole moment which is a linear function of the local field [14]. If a Cartesian component of the field due to the permanent multipole moments is E_a^i, then the induced moment μ_a^i in atom i is

$$\mu_a^i = \alpha^i \left(E_a^i + \sum_{j(\neq i)}^{N} T_{ab}^{ij} \mu_b^j \right) \qquad (1)$$

where α^i is the polarizability of atom i and T_{ab}^{ij} is the symmetrical field gradient tensor, $T_{ab}^{ij} = (1/e)\nabla_a^i E_b^j$, e is the charge of the proton and the subscripts a, b, c, ... are standing for the Cartesian components x, y, z. The expression in parentheses is the total electric field at atom i, consisting of the external field plus the fields of all the other induced dipoles in the molecule.

The set of coupled linear equations (Eq. (1)) for the induced dipole moments can conveniently be expressed in compact matrix equation form, if one introduces the $3N \times 3N$ matrices $\overline{\overline{T}}$ and $\overline{\overline{\alpha}}$, with elements T_{ab}^{ij} and $\alpha_{ab}^i \delta^{ij}$ (δ^{ij} being the Kronecker δ), respectively. In order to suppress the restriction in the sum, the elements T_{ab}^{ij} are defined as zero. Similarly, $\overline{E}$ and $\overline{\mu}$ are $3N \times 1$ column vectors with elements E_a^i and μ_a^i. Eq. (1) is thus written in matrix form,

$$\overline{\mu} = \overline{\overline{\alpha}}\left(\overline{\overline{I}}\,\overline{E} + \overline{\overline{T}}\,\overline{\mu}\right) = \overline{\overline{\alpha I}}\,\overline{E} + \overline{\overline{\alpha T}}\,\overline{\mu}$$

where $\overline{\overline{I}}$ is the $3N \times 3N$-dimensional unit matrix. This matrix equation can be solved for the induced dipoles as

$$\overline{\mu} = \left(\overline{\overline{I}} - \overline{\overline{\alpha T}}\right)^{-1} \overline{\overline{\alpha}}\,\overline{E} = \overline{\overline{A}}\,\overline{E}$$

Here the symmetrical many-body polarizability matrix, $\overline{\overline{A}}$ has been introduced:

$$\overline{\overline{A}} = \left(\overline{\overline{I}} - \overline{\overline{\alpha T}}\right)^{-1} \overline{\overline{\alpha}}$$

It is important to emphasize that the many-body polarizability matrix describes a non-local polarizability response of the system [12]. In effect, an electrostatic field at point j gives rise not only to an induced moment at j (proportional to the diagonal block element A_{ab}^{jj}) but it contributes (*non-locally*) to the induced moments of all the other sites as well.

It should be noted that accurate experimental data on the electronic polarizabilities of molecules, $\overline{\overline{\alpha}}$, are very rare, especially if one is interested in the whole tensor quantity instead of the usual mean value. It seems that modern theoretical chemistry, with the help of powerful computers, is now able to become a substitute for difficult experimental determinations.

A fully operative version of the POLAR program including the whole interacting induced dipoles polarization model [10–14] has been implemented into the MM2 program for molecular mechanics [15,16]. We have called the new version MMID [10–12]. In addition, the polarization energy can be now estimated by three options: (1) no polarization (this option has been introduced for compatibility); (2) non-interacting induced dipoles polarization model (a simplified version where the induced dipoles do not produce further induced dipoles); (3) inter-

acting induced dipoles polarization model (method of Applequist [10–14]).

The MMID algorithm allows three options for selecting which atoms interact, either between atoms: (1) atoms placed at 1–2 (bonded) and further interactions, (2) atoms placed at 1–3 (β neighbors) and further interactions, and (3) atoms placed at 1–4 (γ neighbors) and further interactions, or between bonds and atoms: (1) bond between atoms placed at 1–2 with atom placed at 2 (one of the two atoms of the bond) and further interactions, (2) bond between atoms placed at 1–2 with atom placed at 3 (α neighbor) and further interactions, and (3) bond between atoms placed at 1–2 with atom placed at 4 (β neighbor) and further interactions. The program allows two options of atomic polarizability data bases: (1) atomic polarizabilities from the PAPID program data base [17], (2) atomic polarizabilities from experimental data.

4. Geometrical descriptors and topological indices

The TOPO program for the theoretical simulation of the molecular shape has been described elsewhere [4,5]. Molecular shape is characterized by a set of electrostatic and geometrical descriptors and topological indices [18–22], including the fractal dimension of the solvent accessible surface [23,24]. Atom-to-atom analyses of the descriptors have been implemented [4,5].

The molecular surface of molecules can be represented by the external surface of a set of overlapping spheres with appropriate radii, centered on the nuclei of the atoms. If the radii are those of van der Waals [25], the bare molecular surface is obtained [18,19]; if the radii are those of van der Waals plus the effective radius of a solvent molecule, the solvent accessible molecular surface is now obtained [20].

The theoretical simulation of the molecular shape is helped by the calculation of geometrical descriptors and topological indices of the molecules. The calculations are based on a numerical method proposed by Meyer [18,19]. The molecule is treated as a solid in space defined by tracing spheres about the atomic nuclei. It is computationally enclosed in a graduated rectangular box and the geometrical descriptors evaluated by counting points within the solid or close to chosen surfaces. The molecular volume, V, is concurrently approximated as $V = P \cdot \mathrm{GRID}^3$, where P is the number of points within the molecular volume (within distance R_X of any atomic nucleus X) and GRID is the size of the mesh grid.

As a first approximation, the bare molecular surface area could be calculated as $S = Q \cdot \mathrm{GRID}^2$, where Q is the number of points close to the bare surface area (within a distance between R_X and $R_X + \mathrm{GRID}$ of any atomic nucleus X). However, the estimate has been improved [19]: if the point falls exactly on the surface of one of the atomic spheres, it accounts indeed for GRID^2 units of area on the bare molecular surface. This is because the total surface of atom X can accommodate $4\pi R_X^2/\mathrm{GRID}^2$ points. When a point falls beyond the surface, it represents GRID^2 units of area on the surface of a sphere of radius $R > R_X$, not on the surface of atom X. On the surface of X it accounts only for a fraction of this quantity, namely, $\mathrm{GRID}^2(R_X/R)^2$. The total bare surface area is, therefore, calculated as $S = F \cdot \mathrm{GRID}^2$, where F is the sum of elements AF defined as $\mathrm{AF} = R_X^2/R^2(I)$ for those points close enough to the surface of any atom X. R_X^2 is the squared radius of atom X and $R^2(I)$ is the squared distance of point I from the atomic nucleus X.

Two topological indices of molecular shape can be now calculated: G and G' [19]. The ratio $G = S_e/S$ has been interpreted as a descriptor of molecular globularity; S_e is the surface area of a sphere of volume equal to the molecular volume, V. The ratio $G' = S/V$ has been interpreted as a descriptor of molecular rugosity.

The importance of the solvent validates the assumption that the properties of the systems solvated in water are strongly related to the

contact surface between solute and water molecules [20,22]. We can propose a new molecular geometrical descriptor that is the solvent accessible surface AS [20]. This surface is denoted when a spherical probe is allowed to roll on the outside while maintaining contact with the bare molecular surface. The continuous sheet defined by the locus of the center of the probe is the accessible surface. Alternately, the accessible surface is calculated as the bare molecular surface by using pseudo-atoms, whose van der Waals radii were increased by the radius, R, of the probe.

Fractal surfaces [23] provide a means for characterizing the irregularity of molecular surfaces [24]. The area of the accessible surface, AS, depends on the value of the probe radius, R. The fractal dimension, D, of the molecules may be obtained according to Lewis and Rees [24] as

$$D = 2 - \frac{d(\log \mathrm{AS})}{d(\log R)}$$

An almost fully operative version of the TOPO program has been implemented into the AMYR program for the theoretical simulation of molecular associations and chemical reactions [26–30]. The algorithm allows for the characterization of the molecular units and aggregates. All the geometrical descriptors and topological indices but fractal dimension can be now calculated.

5. Solubilities and partition coefficients

Lipophilic parameters are a measure of the preference of a solute between two solvents [31]. These parameters are quite numerous and have different characters: the parameter of Hansch [32–38], the parameter π-SCAP [31,39], the parameter PARACHOR [40,41], the parameter CSA (cavity surface area) [21], etc.

The lipophilic parameter of Hansch [32], π_X, can be calculated from the partition coefficients of the molecules between two solvents (generally n-octanol and water). The parameter π_X can be defined as

$$\pi_X = \log \frac{P_X}{P_H}$$

where P_X is the partition coefficient of the molecule substituted by X and P_H is the partition coefficient of the reference molecule, measured in the same experimental conditions. The n-octanol–water couple is the most used solvent system and the parameters π_X are relative to this system. Hansch and Leo [32] have tabulated the π_X values for a great number of substituents.

Additional attempts have been carried out to fragment the partition coefficient in order to obtain a system of increments by atoms or by groups of atoms [33–35]. A new method has been proposed by Hopfinger [36,37] to calculate log P. This method is called π-SCAP (solvent-dependent conformational analysis program) and has been initially used to calculate the Gibbs free energy of solvation of macromolecules. From these data, one can calculate $\log P = 0.17567(\Delta G_{\mathrm{solv,w}} - \Delta G_{\mathrm{solv,o}})$ where $\Delta G_{\mathrm{solv,w}}$ and $\Delta G_{\mathrm{solv,o}}$ (in kJ mol^{-1}) are the Gibbs free energies of solvation of the molecule, considered in water and in n-octanol, respectively.

The model used [36,37] is based on the concept of the hydration sphere [38]. The molecule is fragmented into groups of atoms. The starting hypothesis is that one can center, independently on each group of the solute molecule, a solvation sphere. The size of this sphere depends on the solvent and on the group considered. This sphere is occupied by a certain number of solvent molecules. A variation of free energy, due to the extraction of a solvent molecule, is associated with each hydration sphere.

The intersection volume, V°, between the solvation sphere and the van der Waals spheres of the remaining atoms (not bonded to the group under consideration) in the molecule is calcu-

lated. This volume allows for evaluating the effective volume of hydration of the group for a given conformation of the studied molecule. So, the model has four parameters per solvent: (1) n: maximum number of solvent molecules allowed to fill the solvation sphere; (2) Δg: variation of Gibbs free energy associated with the extraction of one solvent molecule out of the solvation sphere; (3) R_v: radius of the hydration sphere; (4) V_f: free volume available for a solvent molecule in the solvation sphere. One also has V_s: volume of the solvent molecule.

The calculations of n, R_v and Δg can be obtained from the minimization of the configuration energy in a force field model [36]. Alternately, the Δg *empirical* values calculated by Gibson and Scheraga [38] are used.

The calculation of V_f is described as follows. In the hydration sphere, part of the volume is excluded to the solvent molecules. This volume consists of the van der Waals volume of the group at which the sphere is centered and of a volume representing the groups bonded to the central group. This later volume is represented by a number of cylinders equal to the number of atoms bonded to the central group and where the axes pass by the center of the sphere. The radius of these cylinders is taken as 3/4 of the van der Waals radius of the central group and these cylinders are disposed in such a way to respect the valence geometry of the group (sp^2, sp^3, ...).

The difference between the total volume of the hydration sphere and the volume excluded to the solvent molecules represents the volume, V', that is really available for the solvent molecules. So, V_f can be calculated as

$$V_f = \frac{V'}{n} - V_s$$

The variation of Gibbs free energy associated with the extraction of all the solvent molecules out of the solvation spheres of a group is

$$\Delta G_R = n\Delta g\left(1 - \frac{V^\circ}{V'}\right)$$

and the variation of the Gibbs free energy associated with the extraction of all the solvent molecules out of the solvent spheres of a molecule is the sum of the Gibbs free energies, ΔG_R, of each group making up the molecule:

$$\Delta G_{extr} = \sum_{R=1}^{N} \Delta G_R$$

The solvation energy of a molecule is the opposite value of this Gibbs free energy:

$$\Delta G_{solv} = -\Delta G_{extr}$$

Though this is a simple method we have found important difficulties in calculating the volume V'. The calculated values are very different from those given by Hopfinger [36,37]. For example one can consider the (CH) aromatic group. It should be noted that the value of V_f in the method of Hopfinger is treated as a fitting parameter. The parameters of Hopfinger in water ($V_s = 21.2$ Å^3) are: $n = 3$, $\Delta g = 0.11$ kcal mol^{-1}, $R_v = -3.9$ Å, $V_f = 3.3$ Å^3, $V' = 76.6$ Å^3 [37].

The calculation of V' with the procedure indicated by Hopfinger [36] follows. Volume of the hydrated sphere: 248.5 Å^3. The CH group has a contact radius of 1.65 Å. Thus, the volume of the CH group is 18.8 Å^3. There are two cylinders of $3.9 - 1.65 = 2.25$ Å of length and $(3/4)1.65 = 1.24$ Å of radius. Thus, the volume of the cylinders is 21.7 Å^3. $V' = 248.5 - 18.8 - 21.7 = 208$ Å^3 and $V_f = 48.1$ Å^3, a very different value of that given by Hopfinger.

This is the most drastic case and represents a relative error of -93%. In all cases but one (the fluorine atom, $E_r = +29\%$) the parametric value of V_f given by Hopfinger underestimates the calculated value, being the mean relative error -46%. In these conditions for the coherence of the calculations, we suggest to evaluate the values of V_f by making use of a computer program. Pascal [31] has written a program called SCAP which makes use of the sub-program KOROBO (that allows for the calculation of the surfaces and volumes by the method of Korobov [39]) in order to calculate the volume V' and evaluate the Gibbs free energies of

Table 1
Electrostatic properties of the molecules

Molecule	μ (D) [a]	Θ (DÅ) [b]	Θ_1 (DÅ) [c]	Θ_2 (DÅ)	Θ_3 (DÅ)	q_M (e) [d]	q_M(ref) (e) [e]
H_2Por	0.063	21.401	0.468	10.358	53.377	0.176	0.231
Fe^{III}Por	0.076	9.384	−11.389	0.005	39.536	2.848	2.909
Mn^{III}Por	0.064	7.498	−14.229	0.000	36.725	3.181	2.909
Fe^{III}PorCl	2.048	−13.812	−54.884	3.767	9.680	2.142	2.783
Mn^{III}PorCl	1.159	−16.232	−57.738	2.201	6.840	2.559	2.783

[a] Dipole moment (debye).
[b] Mean quadrupole moment (debye ångström).
[c] Quadrupole moment tensor eigenvalues Θ_1, Θ_2 and Θ_3 (debye ångström).
[d] Charge of the metal atom (electron charge). In the case of porphin results refer to each H atom.
[e] Reference: Extended Hückel calculation.

solvation in water and in *n*-octanol as well as the partition coefficient.

6. Results and discussion

The electrostatic properties of the molecules are reported in Table 1. The chlorine atom is responsible for the existence of a dipole moment, μ, in the range 1.2–2.0 D for the M^{III}(Por)Cl molecules. Starting from the porphin molecule (Θ about 21 DÅ), the presence of the metal atom decreases the mean value of the quadrupole moment to the range 7–9 DÅ and the addition of the chlorine atom changes the sign of the mean quadrupole moment (in the range −16–(−14) DÅ). This is due to the negative value of the first eigenvalue, Θ_1, of the quadrupole moment tens or for M^{III}(Por)Cl (in the range −58–(−55)DÅ). The atom-to-atom partition of the electrostatic properties reveals that the charge of the metal atom, q_M, (in the range 2.8–3.2 e) is rather varied by the addition of the chlorine atom (to the range 2.1–2.6 e). The charge values vary in the same way as extended Hückel calculations taken as reference (in the range 2.8–2.9 e). The charge values for porphin ($q_H = 0.176$ e) lie in the range of extended Hückel with charge iteration ($q_H = 0.181$ e), CNDO ($q_H = 0.138$ e), INDO ($q_H = 0.133$ e) and ab initio STO-3G ($q_H = 0.298$ e) reference calculations.

The mean value of the molecular polarizability, α, increases with the number of heavy atoms in the molecule (see Table 2). The atom-to-atom partition reveals that the effective polarizability of the metal atom, α_M, (in the range 2.8–2.9 Å^3) is increased by the addition of the chlorine atom (to the range 3.5–3.6 Å^3). The molecular polarizability for porphin ($\alpha = 71.362$ Å^3, $\alpha_1 = 70.702$ Å^3, $\alpha_2 = 71.463$ Å^3, $\alpha_3 = 71.922$ Å^3 $\alpha_H = 0.151$ Å^3, $\alpha_{H1} = 0.038$ Å^3, α_{H2}

Table 2
Molecular polarizability of the molecules

Molecule	α (Å^3) [a]	α_1 (Å^3) [b]	α_2 (Å^3)	α_3 (Å^3)	α_M (e) [c]	α_{M1} (Å^3) [d]	α_{M2} (Å^3)	α_{M3} (Å^3)
H_2Por	71.362	70.702	71.463	71.922	0.151	0.038	0.132	0.282
Fe^{III}Por	77.947	72.071	80.711	81.058	2.756	0.797	3.730	3.741
Mn^{III}Por	78.185	72.085	81.059	81.412	2.931	0.828	3.978	3.988
Fe^{III}PorCl	81.475	73.595	84.329	86.500	3.454	1.119	4.589	4.655
Mn^{III}PorCl	81.720	73.613	84.668	86.879	3.608	1.150	4.802	4.873

[a] Mean molecular polarizability (ångström^3).
[b] Molecular polarizability tensor eigenvalues α_1, α_2 and α_3 (ångström^3).
[c] Effective polarizability of the metal atom (ångström^3). In the case of porphin results refer to each H atom.
[d] Effective polarizability tensor eigenvalues α_{M1}, α_{M2} and α_{M3} for the metal atom (ångström^3).

Table 3
Geometrical descriptors of the molecules

Molecule	V (Å^3) [a]	V(ref) [b]	S (Å^2) [c]	S(ref) [b]	AS (Å^2) [d]	AS(ref) [b]	HBAS [e]	HLAS [f]	AS′ (Å^2) [g]	AS′(ref) [b]
H_2Por	296.1	328.7	306.51	352.62	483.90	527.33	456.38	27.52	912.42	967.31
Fe^{III}Por	287.8	320.2	297.17	341.04	473.05	518.04	452.62	20.43	900.45	955.33
Mn^{III}Por	287.9	320.1	296.85	340.72	473.70	518.25	453.42	20.28	900.81	954.20
Fe^{III}PorCl	307.0	339.6	315.89	360.71	487.80	532.17	436.71	51.09	917.12	969.45
Mn^{III}PorCl	307.0	339.6	315.94	360.72	488.32	531.81	437.07	51.25	914.99	969.07

[a] Molecular volume (ångström^3).
[b] Reference: calculations carried out with the GEPOL program.
[c] Molecular surface area (ångström^2).
[d] Water accessible surface area (ångström^2).
[e] Hydrophobic accessible surface area (ångström^2).
[f] Hydrophilic accessible surface area (ångström^2).
[g] Side-chain accessible surface area (ångström^2).

$= 0.132$ Å^3, $\alpha_{H3} = 0.282$ Å^3) is in the same order of magnitude of reference calculations carried out with the PAPID program [17] that uses a data base of atomic polarizabilities built up from Goupled Hartree–Fock calculations of the polarizability tensors of a series of molecules containing the main functional groups which are present in peptides ($\alpha = 46.205$ Å^3, $\alpha_1 = 20.905$ Å^3, $\alpha_2 = 58.577$ Å^3, $\alpha_3 = 59.135$ Å^3, $\alpha_H = 0.103$ Å^3, $\alpha_{H1} = 0.063$ Å^3, $\alpha_{H2} = 0.112$ Å^3, $\alpha_{H3} = 0.135$ Å^3).

The calculation of the geometrical descriptors and topological indices of Tables 3 and 4 are compared with reference calculations carried out with the GEPOL (GEometry of POLyhedron) program [42]. The GEPOL program has been developed in this laboratory. This program calculates the envelope surface for a molecule, as a point distribution, and computes its correspondent area and volume.

The GEPOL program calculates three kinds of envelope surfaces: (1) The van der Waals molecular surface which is the external surface resulting from a set of spheres centered on the atoms or groups of atoms forming the molecule; (2) the solvent accessible surface which is the surface generated by the center of the solvent, considered as a rigid sphere, when it rolls around the van der Waals surface [20]; (3) the molecular surface which is composed of two parts: the contact surface and the re-entrant surface. The contact surface is the part of the van der Waals surface of each atom which is accessible to a probe sphere of a given radius. The re-entrant surface is defined as the inward-facing part of the probe sphere when this is simultaneously in contact with more than one atom.

For the calculation of the molecular surfaces each sphere is subsequently divided into triangles by a series of tessellations by projecting a pentakis dodecahedron onto each sphere and the surface is obtained by summing up all triangles. The centers and normal vectors of these triangles allow for the graphic representation of scalar and vector molecular properties over the molecular surfaces. The GEPOL program is very fast and efficient.

The geometrical descriptors of the molecules are listed in Table 3. Starting from the porphin molecule, the presence of the metal atom de-

Table 4
Topological indices of the molecules

Molecule	G [a]	G (ref) [b]	G' (Å^{-1}) [c]	G' (ref) [b]	D [d]	D (ref) [b]	D' [e]
H_2Por	0.701	0.653	1.035	1.073	1.38	1.41	1.45
Fe^{III}Por	0.709	0.664	1.033	1.065	1.38	1.41	1.44
Mn^{III}Por	0.710	0.664	1.031	1.064	1.38	1.41	1.44
Fe^{III}PorCl	0.697	0.653	1.029	1.062	1.39	1.42	1.45
Mn^{III}PorCl	0.697	0.653	1.029	1.062	1.39	1.42	1.45

[a] Molecular globularity.
[b] Reference: calculations carried out with the GEPOL program.
[c] Molecular rugosity (ångström^{-1}).
[d] Fractal dimension of the solvent accessible surface.
[e] Fractal dimension of the solvent accessible surface averaged for non-buried atoms.

creases the molecular volume, V, and the addition of the chlorine atom increases the volume. The values are in line with reference calculations carried out with the GEPOL program [42]. The behavior of the molecular surface area, S, the water accessible surface area, AS, and its hydrophilic contribution, HLAS, is the same as has been noticed for the molecular volume. However, the effect is strongly observed in the hydrophilic accessible surface area because the central hydrogen atoms in porphin and the chlorine atom in M^{III}(Por)Cl are polar atoms and contribute to the hydrophilic accessible surface area. The same trend is observed for the side-chain accessible surface area, AS′.

The comparison between the TOPO and GEPOL programs has a special interest because the later does not allow an atom-to-atom partition analysis of the geometrical descriptors and topological indices. Our method (TOPO) allows this atom-to-atom analysis (e.g., contribution to the molecular volume, molecular surface area, molecular globularity, molecular rugosity, water accessible surface area, etc., see Table 5).

For example, after the water accessible surface area is divided into its atomic contributions, the hydrophobic accessible surface area (HBAS) is obtained by summing up the accessible surface areas of non-polar atoms (peripheral H, C, ...) and the hydrophilic accessible surface area (HLAS) is calculated by summing up the accessible surface areas of the polar atoms (central H, N, ...), see Table 3. A large value of HLAS favors the solubility in water which is fundamental for the processability of the material.

The topological indices of the molecules are reported in Table 4. The molecular globularity index, G, is maximal for the metal porphyrin and minimal for the chlorine derivative. The values are in line with reference calculations carried out with the GEPOL program [42]. The molecular rugosity index, G', is maximal for the metal-free porphin molecule. The fractal dimension of the solvent accessible surface, D, (in the range 1.38–1.39) and the fractal dimension averaged for non-buried atoms, D', (in the range 1.44–1.45) are slightly varied by the presence of the metal and chlorine atoms.

The atom-to-atom partition for the metal atom of the geometrical descriptors and topological indices of the molecules are summarized in Table 5. In the case of porphin, results are referred to each H atom. The contribution of the metal atom to the molecular volume, V, and surface area, S, is decreased by the addition of the chlorine atom. The molecular globularity at the surface of the metal atom, G, is maximal for the chlorine derivative. However, the molecular rugosity at the surface of the metal atom, G', is

Table 5
Geometrical descriptors and topological indices of the molecules: atom-atom partition for the metal atom

Molecule	V (Å^3) [a]	S (Å^2) [b]	G [c]	G' (Å^{-1}) [d]	AS (Å^2) [e]	Accessibility [f]	D' [g]
H_2Por	7.3	7.64	2.370	1.055	8.40	0.093	1.73
Fe^{III}Por	4.3	3.42	3.747	0.793	1.11	0.015	6.22
Mn^{III}Por	4.5	3.57	3.706	0.789	1.32	0.017	6.10
Fe^{III}PorCl	3.9	1.72	6.987	0.439	0.63	0.008	— [h]
Mn^{III}PorCl	4.1	1.78	7.004	0.431	0.73	0.010	— [h]

In the case of porphin, results refer to each H atom.
[a] Molecular volume (ångström^3).
[b] Molecular surface area (ångström^2).
[c] Molecular globularity.
[d] Molecular rugosity (ångström^{-1}).
[e] Water accessible surface area (ångström^2).
[f] Accessibility of the accessible surface.
[g] Fractal dimension of the solvent accessible surface.
[h] A dash indicates that the atom is buried and the fractal dimension cannot be calculated.

Table 6
Solvation descriptors of the molecules

Molecule	$\Delta G_{solv,w}$ [a]	$\Delta G_{solv,o}$ [b]	log P [c]	$V_{cav,w}$ [d]	$S_{cav,w}$ [e]	$V_{cav,o}$ [f]	$S_{cav,o}$ [g]
H_2Por	−31.42	−62.57	5.48	1222.0	600.46	3452.4	1154.40
Fe^{II}Por	−25.62	−59.73	6.00	1474.3	650.54	3462.4	1143.08
Mn^{II}Por	−25.48	−59.65	6.01	1468.0	647.89	3446.5	1139.78
Fe^{III}PorCl	−25.97	−61.20	6.19	1469.5	647.01	3516.7	1152.55
Mn^{III}PorCl	−25.99	−61.19	6.19	1490.7	657.11	3532.0	1158.01

[a] Gibbs free energy of solvation in water (kJ mol^{-1}).
[b] Gibbs free energy of solvation in *n*-octanol (kJ mol^{-1}).
[c] P is the *n*-octanol–water partition coefficient.
[d] Cavity volume in water (ångström^3).
[e] Cavity surface area in water (ångström^2).
[f] Cavity volume in *n*-octanol (ångström^3).
[g] Cavity surface area in *n*-octanol (ångström^2).

minimal for the chlorine complex. The trend of the contribution of the metal atom to the accessible surface area, AS, is the same as has been seen for the molecular surface area. The accessibility of the metal atom surface in the metal porphyrin is about 1.6% and decreases to about 0.9% for the chlorine derivative. The fractal dimension for the metal atom solvent accessible surface, D', takes a very high value in the range 6.1–6.2 when compared with the molecular value averaged for non-buried atoms ($D' = 1.44$ in the last column of Table 4). This means that the irregularity of the molecular surface is maximal at the metal atom solvent accessible surface.

The solvation descriptors of the molecules are reported in Table 6. In the case of MPor results are referred to the M^{II}Por non-charged molecule. Starting from the porphin molecule, the absolute values of the Gibbs free energies of solvation in water, $|\Delta G_{solv,w}|$, and in *n*-octanol, $|\Delta G_{solv,o}|$, are decreased by the presence of the metal atom and increased by the addition of the chlorine atom. This last variation is explained by an increase in the hydrophilic accessible surface area (see Table 3). The result is that the *n*-octanol–water partition coefficient is minimal for the metal free porphin (log $P = 5.48$) and maximal for the chlorine porphyrin derivative (log $P = 6.19$). The cavity volume, $V_{cav,w}$, and surface area in water, $S_{cav,w}$ are minimal for the metal free porphin, and maximal for the metal porphyrin molecule and the chlorine porphyrin complex. The cavity volume, $V_{cav,o}$, and surface in *n*-octanol, $S_{cav,o}$, are minimal for the metal-free porphin and metal porphyrin, and maximal for the chlorine derivative.

A fully operative version of the POLAR program has been implemented into the MM2 program for molecular mechanics [10–12,15,16]. An almost fully operative version of the TOPO program has been implemented into the AMYR program for the theoretical simulation of molecular associations and chemical reactions [26–30].

In this paper we have reported the calculation of molecular dipole moments, $\bar{\mu}$, tensor quadrupole moments, $\bar{\bar{\Theta}}$, and polarizabilities, $\bar{\bar{\alpha}}$, which we have successfully applied to porphin, iron and manganese porphyrins and their chlorine derivatives. Although these values are quantitatively inaccurate for predicting high-temperature frequency-dependent $\bar{\bar{\alpha}}$ polarizabilities of condensed phases, they may prove useful in predicting relative properties for different systems. This work represents a first step for modelling catalyzed saturated alkane hydroxylations.

References

[1] P.R. Ortiz de Montellano (Ed.), Cytochrome P-450: Structure, Mechanism and Biochemistry, Plenum Press, New York, 1986.
[2] B. Meunier, Chem. Rev. 92 (1992) 1411–1456.

[3] A. Sorokin, A. Robert and B. Meunier, J. Am. Chem. Soc. 115 (1993) 7293–7299.
[4] F. Torrens, E. Ortí and J. Sánchez-Marín, J. Chim. Phys. Phys. Chim. Biol. 88 (1991) 2435.
[5] F. Torrens, E. Ortí and J. Sánchez-Marín, in: M. Durand and F. El Dabaghy (Eds.), High Performance Computing II, North-Holland, Amsterdam, 1991, p. 549.
[6] R.T. Sanderson, Science 114 (1951) 670.
[7] S.G. Bratsch, J. Chem. Edu. 61 (1984) 588.
[8] R.S. Mulliken, J. Chem. Phys. 2 (1934) 782.
[9] J.E. Huheey, J. Phys. Chem. 69 (1965) 3284.
[10] F. Torrens, C. Voisin and J.-L. Rivail, in: R. Glowinsky (Ed.), Computing Methods in Applied Sciences and Engineering, Nova Science, New York, 1991, p. 249.
[11] F. Torrens, M. Ruiz-López, C. Cativiela, J.I. García and J.A. Mayoral, Tetrahedron 48 (1992) 5209.
[12] F. Torrens, J. Sánchez-Marín and J.-L. Rivail, An. Fís. Madrid 90 (1994) 197.
[13] L. Silberstein, Philos. Mag. 33 (1917) 92.
[14] J. Applequist, J.R. Carl and K.K. Fung, J. Am. Chem. Soc. 94 (1972) 2952.
[15] N.L. Allinger, J. Am. Chem. Soc. 99 (1977) 8127.
[16] N.L. Allinger and Y.H. Yuh, MM2, QCPE Program No. 395.
[17] C. Voisin, A. Cartier and J.-L. Rivail, J. Phys. Chem. 96 (1992) 7966.
[18] A.Y. Meyer, J. Chem. Soc. Perkin Trans. 2 (1985) 1161.
[19] A.Y. Meyer, J. Comput. Chem. 9 (1988) 18.
[20] B. Lee and F.M. Richards, J. Mol. Biol. 55 (1971) 379.
[21] R.B. Hermann, J. Phys. Chem. 76 (1972) 2754.
[22] S.J. Wodak and J. Janin, Proc. Natl. Acad. Sci. USA 77 (1980) 1736.
[23] B.B. Mandelbrot, The Fractal Geometry of Nature, Freeman, San Francisco, 1983.
[24] M. Lewis and D.C. Rees, Science 230 (1985) 1163.
[25] A. Bondi, J. Phys. Chem. 68 (1964) 441.
[26] S. Fraga, J. Comput. Chem. 3 (1982) 329.
[27] S. Fraga, Comput. Phys. Commun. 29 (1983) 351.
[28] F. Torrens, R. Montañana and J. Sánchez-Marín, in: J.L. Delhaye and E. Gelenbe (Eds.), High Performance Computing, North-Holland, Amsterdam, 1989, p. 299.
[29] F. Torrens, E. Ortí and J. Sánchez-Marín, Comput. Phys. Commun. 66 (1991) 341.
[30] F. Torrens, E. Ortí and J. Sánchez-Marín, J. Mol. Graph. 9 (1991) 254.
[31] P. Pascal, Program SCAP, Université de Nancy I (1991).
[32] C. Hansch and A. Leo, Substituent Constants for Correlation Analysis in Chemistry and Biology, Wiley, New York, 1979.
[33] R.F. Rekker, The Hydrophobic Fragmental Constant, Vol. 1, Elsevier, Amsterdam, 1977.
[34] R.F. Rekker and H.M. de Kort, Eur. J. Med. Chem. Chim. Ther. 14 (1979) 479.
[35] J. Moreau, personal communication.
[36] A.J. Hopfinger, Macromolecules 4 (1971) 731.
[37] A.J. Hopfinger and R.D. Battershell, J. Med. Chem. 19 (1976) 569.
[38] K.D. Gibson and H.A. Scheraga, Proc. Natl. Acad. Sci. USA 58 (1967) 420.
[39] P. Claverie, J. Phys. Chem. 76 (1972) 2123.
[40] O.R. Quayle, Chem. Rev. 53 (1953) 439.
[41] McGowan, Recl. Trav. Chim. Pays-Bas 75 (1956) 193.
[42] J.L. Pascual-Ahuir, E. Silla, J. Tomasi and R. Bonaccorsi, GEPOL, QCPE Program No. 554 (1988).